Bone 54 (2013) 44–47

Contents lists available at SciVerse ScienceDirect

Bone

journal homepage: www.elsevier.com/locate/bone

Technical Note

Direct depiction of bone microstructure using MRI with zero echo time ☆

Markus Weiger [a,b,c,*], Marco Stampanoni [c,d], Klaas P. Pruessmann [c]

[a] Bruker BioSpin AG, Faellanden, Switzerland
[b] Bruker BioSpin MRI GmbH, Ettlingen, Germany
[c] Institute for Biomedical Engineering, University and ETH Zurich, Zurich, Switzerland
[d] Swiss Light Source, Paul Scherrer Institute, Villigen, Switzerland

ARTICLE INFO

Article history:
Received 27 July 2012
Revised 27 December 2012
Accepted 16 January 2013
Available online 26 January 2013

Edited by: Harry Genant

Keywords:
ZTE
Short T2
Bone matrix
Bone water
Bone marrow

ABSTRACT

This paper reports a proof of principle of direct depiction of trabecular bone microstructure in vitro by means of magnetic resonance imaging (MRI). Such depiction is achieved by ^{1}H imaging of water embedded in the bone matrix. The fast transverse relaxation of this compartment with T_2^* on the order of a few hundreds of microseconds is addressed by a three-dimensional MRI technique with zero echo time (ZTE). ZTE imaging at an isotropic spatial resolution of 56 μm is demonstrated in a trabecular bone specimen extracted from a bovine bone. In the MR images, the trabecular bone structure is clearly depicted and a high level of robustness against off-resonance artefacts is observed. The structural accuracy of the MR data is investigated by comparison with x-ray micro-computed tomography.

Introduction

The characterisation of osteoporosis is usually based on measurement of bone mineral density (BMD) by means of dual-energy x-ray absorptiometry. However, it has been found that the BMD value is not sufficient as an indicator of osteoporosis and information about the bone micro-architecture enables improved classification [1]. Moreover, knowledge of the degree of mineralisation of the bone (DMB) is the basis for differentiating between osteoporosis and osteomalacia [2]. To further investigate these relationships, the microstructure of bone has been determined in vitro in extracted samples and in vivo both with x-ray [1,3] and with magnetic resonance imaging (MRI) techniques [4,5]. Relative to x-ray imaging, MRI has the fundamental advantage of operating without ionising radiation. It also offers a larger range of contrast options and is thus widely used for musculoskeletal diagnostics and research. However, MRI of bone tissue is hampered by low water content and very fast signal decay by T_2^* relaxation [6]. Therefore, all efforts so far to depict bone micro-structure by MRI have relied on negative contrast, which is obtained by imaging exogenous fluids or bone marrow in the trabecular spaces [4,5].

At coarser resolutions, MRI has also been accomplished based on signal from the bone itself, including ^{31}P imaging of the mineral matrix [7–9] and ^{1}H imaging of the water embedded in the bone matrix [10,11]. While the former enables direct quantification of the DMB, the latter provides considerably larger signal-to-noise ratio (SNR) and permits indirect estimates of the DMB based on its inverse relationship to bone water [6,12,13]. The underlying direct MR depiction of bone is usually based on specialised techniques such as ultra-short echo time (UTE) [14], water- and fat-suppressed proton projection MRI (WASPI) [15], or solid-state MRI [16]. So far, the spatial resolutions obtained with these latter techniques have not been sufficient to resolve the trabecular structure without considerable partial volume effects, which hamper the derivation of quantitative structural parameters [17].

The goal of the present work is to overcome this limitation and reconcile direct MR depiction of bone with spatial resolutions suitable for studying trabecular microstructure. This is achieved by adopting recent progress in MRI with zero echo time (ZTE) [18–21], which has been shown to offer superior short-T_2^* capability, high spatial resolution, and high robustness against off-resonance and gradient eddy-current effects. The feasibility of this approach is demonstrated

Abbreviations: 1D, one-dimensional; 3D, three-dimensional; BMD, bone mineral density; DMB, degree of mineralisation of bone; FID, free induction decay; MRI, magnetic resonance imaging; μCT, micro-computed tomography; SNR, signal-to-noise ratio; SRXTM, synchrotron-based x-ray tomographic microscopy; T2, transverse relaxation constant; T2*, apparent transverse relaxation constant; T/R, transmit-receive; UTE, ultra-short echo time; WASPI, water- and fat-suppressed proton projection MRI; ZTE, zero echo time.

☆ Disclosures: MW was an employee of Bruker BioSpin until May 2012. KP receives research support from Philips Healthcare and is a shareholder of Gyrotools LLC and Skope Magnetic Resonance Technologies LLC.

* Corresponding author at: Institute for Biomedical Engineering, University and ETH Zurich, Gloriastrasse 35, CH-8092 Zurich, Switzerland. Fax: +41 44 632 11 93.
E-mail address: weiger@biomed.ee.ethz.ch (M. Weiger).

8756-3282/$ – see front matter © 2013 Elsevier Inc. All rights reserved.
http://dx.doi.org/10.1016/j.bone.2013.01.027

by imaging of a bone sample and verification of the observed trabecular structure by comparison with micro-computed tomography (μCT).

Materials and methods

ZTE imaging

Transverse relaxation of bone water occurs with T_2^* on the order of a few hundred microseconds [6]. Performing MRI of such a sample requires that data acquisition starts as soon as possible after signal excitation. Moreover, signal encoding must be completed roughly within T_2^* to avoid resolution loss due signal decay. In ZTE MRI, these demands are met by employing a purely frequency-encoded, three-dimensional (3D), radial, centre-out encoding scheme with large gradients and hence high bandwidth. Zero echo time is achieved by switching on the projection gradient before RF excitation with a large-bandwidth (i.e. short) hard pulse (Fig. 1) [18,19]. Thus, spatial encoding starts with zero delay (rendering TE equal to zero) and at full *k*-space speed, which is essential for reaching maximal resolution at any given T_2^* and gradient strength. Switching the MRI spectrometer from transmit to receive operation incurs a certain dead time Δ, which includes the pulse duration, the actual transmit-receive (T/R) switching, and the build-up time of the digital acquisition filter [20]. For robust operation, this dead time needs to be kept within few multiples of the acquisition dwell time.

Due to the initial dead time, raw ZTE data is incomplete in the *k*-space centre, requiring special means of image reconstruction. First, using an algebraic approach [22], one-dimensional (1D) projections are reconstructed from pairs of readouts with opposite gradient polarity. In this process, the capability of handling small gaps in the data is based on the signal's known bandwidth limitation and on acquisition oversampling [22], which jointly permit finite-support extrapolation [23]. The 1D projections are then transferred back to *k*-space by 1D Fourier transform and the final 3D image is obtained by standard 3D regridding and Fourier transform.

ZTE was performed on a Bruker μMRI-system equipped with a 7 T vertical standard-bore magnet and an AVII console driven with ParaVision 5.1 software. A Micro5 probe head was used, including a gradient system with a maximum strength of 2880 mT/m and an RF saddle coil with 5 mm diameter and 20 mm length. Considering a trabecular thickness in the range of 100–200 μm [4], an isotropic resolution of 56 μm was chosen, using a matrix size of 144^3. Further imaging parameters were: flip angle 4°, repetition time 1.5 ms, 65,619 radial readouts per average (fulfilling the Nyquist criterion throughout the acquired *k*-space sphere), and 2120 averages, resulting in a total scan time of 58 h. With the selected signal bandwidth of 200 kHz, the readout duration was 360 μs in line with the expected T_2^* of bone water. With respect to the Nyquist dwell time of $dw = 5$ μs, acquisition oversampling by a factor of 4 was employed. With an RF pulse duration of 1 μs, a T/R switching duration of 4.5 μs, and the short digital filter applied [20], the total dead time was $\Delta = 6.875\ \mu s = 1.375\ dw$.

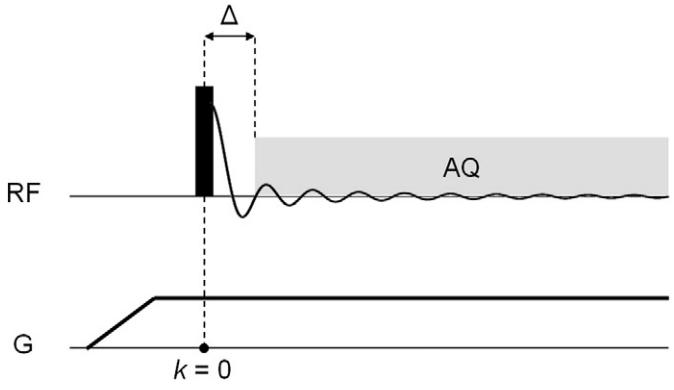

Fig. 1. Scheme of radial centre-out ZTE acquisition. After ramping up the projection gradient, a short, hard RF excitation pulse is applied. The first valid data point is acquired after a dead time Δ due to durations of the RF pulse, T/R switching, and signal build-up of the digital filter.

Micro computed tomography

For reference, high-resolution μCT data were acquired with synchrotron-based x-ray tomographic microscopy (SRXTM) at the TOMCAT beamline of the Swiss Light Source [3]. Using a matrix size of $2048^2 \times 1780$, an isotropic pixel size of 1.85 μm was achieved. The scan time was 5 minutes at an x-ray energy of 17.5 keV.

Processing

Data processing was performed using the FSL software library [24]. In addition to the full-resolution SRXTM data set, the μCT data was down-sampled to an isotropic pixel size of 14.8 μm, corresponding to conventional μCT. For visual comparison, the 3D μMRI data set was co-registered with the μCT data, permitting translations, rotations, and per-axis scaling. The bone signal was identified by image segmentation, thus enabling the calculation of the bone volume fraction.

Bone sample

From a bovine bone, close to a joint an approximately cylindrical piece of about $(4\ mm)^3$ of trabecular bone was extracted. The specimen was dried under ambient conditions and no further treatment was applied.

Results

Initially, using an acquisition without gradient, a free induction decay (FID) was obtained from the whole bone specimen. As in Ref. [6], mainly two components with different relaxation were observed. A bi-exponential fit of the FID provided T_2^* values of 8.7 μs and 290 μs with relative signal contributions of 62% and 38%. Targeting the longer-lived component for imaging, this finding confirmed the readout duration of 360 μs.

The first row of Fig. 2 shows images of the bone specimen obtained with μMRI. Three central orthogonal cross sections, one of axial and two of longitudinal orientation, were selected from the 3D data set. The trabecular micro-architecture is well depicted, confirming sufficient spatial resolution for the ranges of trabecular thickness and spacing present in the sample. The bone matrix exhibits an intermediate signal level whereas bone marrow appears brighter due to higher proton density. The SNR was measured in the images for bone and marrow, resulting in values of 26 and 49, respectively. Large parts of the marrow spaces are empty due to shrinkage upon drying. Despite the lipid chemical shift of about 1000 Hz, owing to the large acquisition bandwidth only minor blurring and no ringing due to off-resonance are observed. Similarly, no significant off-resonance artefacts occur at interfaces between tissues and the surrounding air. The indicated bright artefact arises from a contamination in the probe located in the non-linear range of the gradients, which gave off a very short-T_2^* proton signal. A barely noticeable level of background signal is ascribed to the strongly broadened image of the short-lived signal component observed in the FID.

For comparison, the third row of Fig. 2 shows the corresponding μCT images. Excellent agreement is observed between the two modalities as illustrated by overlaid images in the second row. In addition, a close-up of the SRXTM data at full resolution is shown in the bottom row, exhibiting fine details such as e.g. the lacunae.

Fig. 3 shows 3D-rendered bone representations according to segmentation of the μMRI and μCT data, respectively. The 3D visualisation confirms the successful depiction and segmentation of the bone